Letter

Shedding light on charmonium

Zhiguo Wang,[1] Meijian Li,[2,*] Yang Li,[1] and James P. Vary[3]

[1]*Department of Modern Physics, University of Science and Technology of China, Hefei 230026, China*
[2]*Instituto Galego de Fisica de Altas Enerxias (IGFAE), Universidade de Santiago de Compostela, E-15782 Galicia, Spain*
[3]*Department of Physics and Astronomy, Iowa State University, Ames, Iowa 50011*

(Received 10 December 2023; accepted 6 February 2024; published 29 February 2024)

We investigate E1 radiative transitions within charmonium in a relativistic approach based on light-front QCD. In quantum field theory, two sets of processes are pure E1: $\chi_{c0} \to J/\psi\gamma$ ($\psi \to \chi_{c0}\gamma$) and $h_c \to \eta_c\gamma$ ($\eta_c' \to h_c\gamma$), both involving the P-wave charmonia. We compute the E1 radiative decay widths as well as the corresponding transition form factors of various processes including those involving $2P$ states. These observables provide an access to the microscopic structures of the P-wave charmonium. We show that our parameter-free predictions are in excellent agreement with the experimental measurements as well as lattice simulations whenever available.

DOI: 10.1103/PhysRevD.109.L031902

Introduction. The discoveries of charmoniumlike states, e.g., $\chi_{c1}(3872)$ and $\chi_{c0}(3915)$, have sparked renewed interests in the charmonium structure [1–3]. The proximity of their masses to the $D\bar{D}$ threshold leads to the speculation that at least some of them may be meson molecules [4]. On the other hand, their quantum numbers are consistent with conventional $c\bar{c}$ quark model and their masses are also in the vicinity of the $2P$ charmonia in various quark model predictions [5]. Furthermore, decay patterns from the quark models can encapsulate various coupled channel effects [6–19]. In any case, the investigation of the microscopic structures of charmonium offers new insights into the nature of the strong force, which, after 50 years of QCD, remains one of the biggest puzzles in physics [20].

The radiative transitions provide a clean probe with variable resolutions to the microscopic composition of the system [21–32]. Furthermore, these transitions are sensitive to relativistic effects, which underlines some recent discrepancies between Nonrelativisitic QCD (NRQCD) and the experimental measurements [33–36]. For example, the two-photon decay width in NRQCD converges poorly and deviates from the experimental measurements up to 7σ in next-to-next-to-leading order (NNLO) [35]. A possible explanation is that charmonium is an intrinsically relativistic system. And the relativistic effects are stronger for the excited states. Therefore, a systematic investigation of the radiative transitions for both the ground-state P-wave charmonia and their excitations is required to obtain a complete picture of these charmoniumlike states [33,37,38].

In our previous works, parameter-free predictions are made for the two-photon widths [38] and the M1 widths [39], as well as the associated transition form factors (TFFs). Our results are based on light-front wave functions (LFWFs [40,41]) from basis light-front quantization (BLFQ [42]). This approach is a natural framework to tackle hadrons as relativistic many-body bound states in the nonperturbative regime [43]. For the application to charmonium, two parameters, the charm quark mass m_c and the basis scale κ, were fit to the charmonium mass spectrum [43] (see also Fig. 1). Then the obtained LFWFs are used to make parameter-free predictions to hadronic observables, e.g., decay constants [43], as well as partonic observables, e.g., parton distribution functions [44–48]. All of these results were shown to be in reasonable agreement with the experimental measurements whenever available. We note that rotational symmetry is not explicit in the BLFQ approach but can be calibrated by calculating observables that should be simply related under rotational symmetry operations. Examples of such calibrations within BLFQ have been investigated in terms of mass eigenvalues and radiative transitions in Refs. [39,43].

We focus here on the E1 transitions (Fig. 1) between P-wave scalar charmonia χ_{c0} (0^{++}) and vector charmonia ψ (1^{--}), as well as between P-wave axial vector h_c (1^{+-}) and pseudoscalars η_c (0^{-+}), which are relevant for unraveling the relativistic structure of P-wave charmonium. We assume the states are pure $c\bar{c}$ s. Therefore, any significant deviation from the experimental measurements implies a deviation from the conventional $c\bar{c}$ picture.

The E1 transition has a similar helicity structure scalar-vector-vector with the scalar meson two-photon

*meijian.li@usc.es

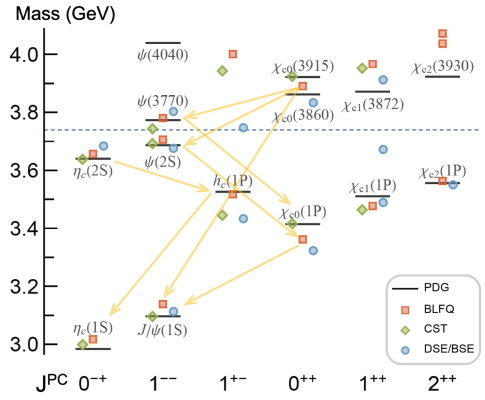

FIG. 1. Schematic view of the pure E1 transitions (yellow arrows) within charmonium. Other radiative transitions, e.g., M1, M2, and E2, are not shown. The masses obtained in BLFQ along with similar relativistic approaches (Covariant spectator theory (CST) [49] and Dyson-Schwinger equations (DSE)/Bethe-Salpeter equations (BSE) [50]) are shown for comparison (see Sec. 5.4 of Ref. [20] and therein). Figure is adapted from Ref. [20].

transition [38]. Since the structures of the photon and vector charmonia are well established, these two processes can be used to constrain the structure of the scalar charmonia at different scales. Figure 2 combines the E1 widths $\Gamma_{S\to V\gamma}$ (or $\Gamma_{V\to S\gamma}$) and the two-photon width $\Gamma_{S\to\gamma\gamma}$ for scalar charmonia $\chi_{c0}(1P)$ and $\chi_{c0}(2P)$, as obtained in BLFQ [38]. Processes for $1P$ scalar χ_{c0} have been measured by several experiments and compiled by PDG [51]. Our results are in good agreement with the PDG values, which provide a

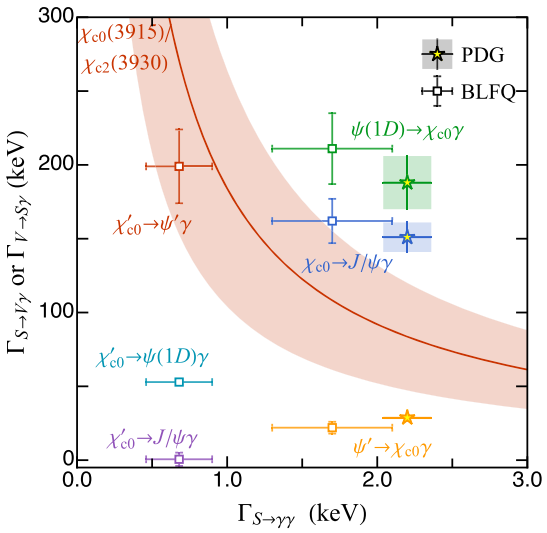

FIG. 2. The BLFQ prediction of scalar charmonium radiative widths $\Gamma_{S\to\gamma\gamma}$ and $\Gamma_{S\to V\gamma}$ as compared with the PDG values [51]. The red curve with a band is the Belle measurement of the product $\Gamma(R\to\psi'\gamma)\Gamma(R\to\gamma\gamma)/\Gamma_{\text{total}} = 9.8(3.6)(1.3)$ eV, where R is identified as $\chi_{c0}(3915)$ or $\chi_{c2}(3930)$ [52]. We take the $N_{\max} = 8$ BLFQ LFWFs to extract the result, and use the difference between it and the $N_{\max} = 16$ result to indicate basis sensitivity; see also in the text.

basis for making predictions for the $2P$ state χ'_{c0}. Experimentally, the only available E1 data come from Belle for $\chi_{c0}(3915)$, a prime candidate for the $2P$ scalar. Last year, Belle collaboration discovered a resonance with the mass 3.922 GeV, which can be identified as $\chi_{c0}(3915)$ or $\chi_{c2}(3930)$. Belle also measured the product $\Gamma(R\to\psi'\gamma)\Gamma(R\to\gamma\gamma)/\Gamma_{\text{total}} = 9.8(3.6)(1.3)$ eV, which is shown as a red curve with a band in Fig. 2 [52]. Our predicted E1 and diphoton widths are consistent with this result.

Formalism. The E1 amplitude of a scalar meson S decaying into a vector meson V plus a (virtual) photon is described by the hadronic matrix element (HME),

$$H_{\lambda_\gamma\lambda'}(q^2) = e\mathcal{Q}_c\varepsilon^{\mu*}_{\lambda_\gamma}(q)\langle V(p',\lambda')|J_\mu(0)|S(p)\rangle, \quad (1)$$

where $J_\mu(x)$ is the current operator, $\mathcal{Q}_c = 2/3$ is the charge number, $e = \sqrt{4\pi\alpha_{\text{em}}}$ is the electron charge, $q = p' - p$ is the four-momentum of the photon, and $\varepsilon^\mu_{\lambda_\gamma}(q)$ is the polarization vector of the photon. Following Ref. [53], we parametrize the HME in terms of its Lorentz structures,

$$\begin{aligned}&\langle V(p',\lambda')|J^\mu(0)|S(p)\rangle\\ &= E_1(Q^2)\left[e^{\mu*}_{\lambda'}(p') - \frac{e^*_{\lambda'}\cdot p}{\Omega(Q^2)}(p'^\mu(p\cdot p') - M_V^2 p^\mu)\right]\\ &\quad + \frac{M_V C_1(Q^2)}{iQ\Omega(Q^2)}(e^*_{\lambda'}\cdot p)\\ &\quad \times[(p\cdot p')(p+p')^\mu - M_S^2 p'^\mu - M_V^2 p^\mu], \end{aligned} \quad (2)$$

where $Q^2 = -q^2$, and $\Omega(Q^2) = (p\cdot p')^2 - M_S^2 M_V^2$. $e^\mu_\lambda(p)$ is the polarization vector of the vector meson. The form factors E_1 and C_1 defined here can be extracted from the transverse and longitudinal amplitudes, respectively, viz.,

$$\begin{aligned}H_{\lambda_\gamma=\pm1,\lambda'} &= e\mathcal{Q}_c E_1(Q^2),\\ H_{\lambda_\gamma=0,\lambda'} &= -e\mathcal{Q}_c C_1(Q^2).\end{aligned} \quad (3)$$

In particular, the E1 radiative decay width is proportional to $|E_1(0)|^2$,

$$\Gamma = \frac{\mathcal{Q}_c^2\alpha_{\text{em}}}{2j_i+1}\frac{M_i^2 - M_f^2}{2M_i^3}|E_1(0)|^2. \quad (4)$$

Here, j_i, M_i are the initial state spin and mass, respectively, and M_f is the final state mass. The vector meson decaying into a scalar plus a photon can be similarly expressed. The Lorentz structures of the HME between pseudoscalar 0^{-+} and the C-odd axial vector 1^{+-} are identical to Eq. (2).

Though in principle, the transition form factors defined in Eqs. (1) and (2) are Lorentz invariant, in practical calculations using valence LFWFs, Lorentz symmetry can be broken since choosing a different current component

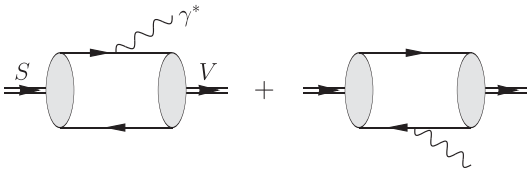

FIG. 3. Leading order diagrams of the E1 radiative transition $S \to V + \gamma^*$.

can lead to a different result—e.g., some choices are more sensitive to small components of the LFWFs which are themselves more sensitive to basis space truncation as observed in M1 transitions [39]. In a nonrelativistic quark model, the E1 transition is induced by the electric dipole interaction. The corresponding electric charge density on the light front is $J^+ = J^0 + J^3$, where we adopt the light-front coordinates $v^\mu = (v^+, v^-, \vec{v}_\perp)$ with $v^\pm = v^0 \pm v^3$ and $\vec{v}_\perp = (v^1, v^2)$. J^+ is also known as the "good current" in light-front dynamics as it is not contaminated by the spurious Lorentz-symmetry violating contributions [54–56]. We further adopt the Drell-Yan frame $q^+ = 0$, which simplifies the expression dramatically [54,56]. The relevant diagrams for the E1 process are shown in Fig. 3. The nonperturbative structures of the initial- and final-state mesons are encoded in the LFWFs,

$$|\psi_h(P, j, m_j)\rangle = \sum_{s,\bar{s}} \int_0^1 \frac{\mathrm{d}x}{2x(1-x)} \int \frac{\mathrm{d}^2 k_\perp}{(2\pi)^3} \psi^{(m_j)}_{s\bar{s}/h}(x, \vec{k}_\perp) \times \frac{1}{\sqrt{N_c}} \sum_i b^\dagger_{si}(p) d^\dagger_{\bar{s}i}(\bar{p})|0\rangle, \tag{5}$$

where $x = p^+/P^+$ is the longitudinal momentum fraction of the quark, and $\vec{k}_\perp = \vec{p}_\perp - x\vec{P}_\perp$ is the relative transverse momentum of the quark. The momenta of the quark and the antiquark are $p^\mu = (xP^+, \vec{k}_\perp + x\vec{P}_\perp)$, $\bar{p}^\mu = ((1-x)P^+, -\vec{k}_\perp + (1-x)\vec{P}_\perp)$. Here, $i = 1, 2, \ldots N_c$ is the color index and $N_c = 3$. The LFWF $\psi^{(m_j)}_{s\bar{s}/h}(x, \vec{k}_\perp)$ is frame independent and only depends on the relative motion of the quark and antiquark. In principle, there are contributions from higher Fock sectors [57–59], which we neglect in the current work. As mentioned, we adopt the approximation that charmonium is pure $c\bar{c}$.

Using the LFWFs, the TFF E1 can be represented as

$$E_1(Q^2) = 4\sum_{s,\bar{s}} \int \frac{\mathrm{d}x}{2x(1-x)} \int \frac{\mathrm{d}^2 k_\perp}{(2\pi)^3} \left\{ M_V \psi^{(\lambda=0)*}_{s\bar{s}/V}(x, \vec{k}_\perp) + \frac{M_S^2 - M_V^2 + Q^2}{\sqrt{2}Q} \psi^{(\lambda=+1)*}_{s\bar{s}/V}(x, \vec{k}_\perp) \right\} \times \psi_{s\bar{s}/S}(x, \vec{k}_\perp + (1-x)\vec{q}_\perp), \tag{6}$$

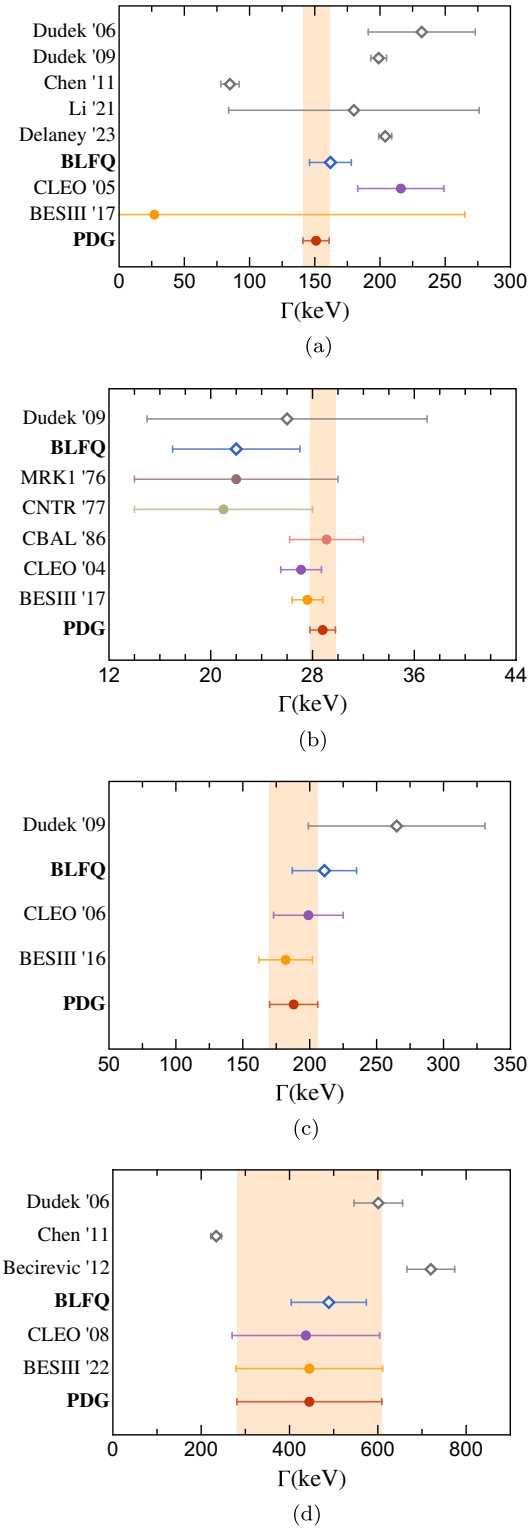

FIG. 4. Comparison of the E1 decay widths from this work (BLFQ) and from the experimental measurements [60–72] including the PDG values [51]. The lattice QCD results [53,74–78] are also shown for comparison. See explanation of the basis sensitivity in the caption of Fig. 2 and in the text. (a) $\chi_{c0} \to J/\psi + \gamma$. (b) $\psi(2S) \to \chi_{c0} + \gamma$. (c) $\psi(3770) \to \chi_{c0} + \gamma$. (d) $h_c \to \eta_c(1S) + \gamma$.

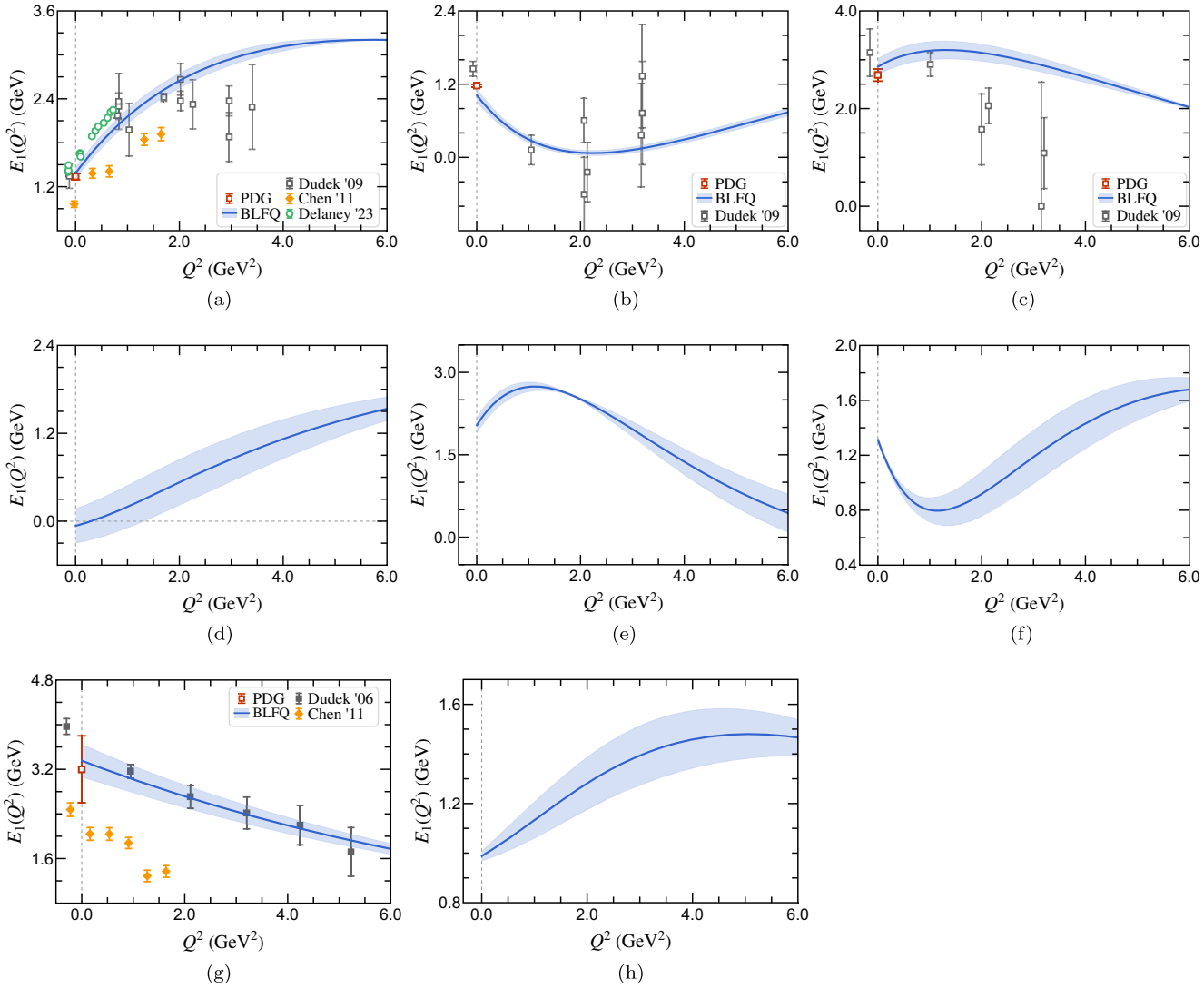

FIG. 5. Comparison of the E1 radiative transition form factors from this work (BLFQ) and from several lattice simulations [53,74,75,78]. See explanation of the basis sensitivity in the caption of Fig. 2 and in the text. (a) $\chi_{c0} \to J/\psi + \gamma$. (b) $\psi(2S) \to \chi_{c0} + \gamma$. (c) $\psi(3770) \to \chi_{c0} + \gamma$. (d) $\chi_{c0}(2P) \to J/\psi + \gamma$. (e) $\chi_{c0}(2P) \to \psi(2S) + \gamma$. (f) $\chi_{c0}(2P) \to \psi(3770) + \gamma$. (g) $h_c(1P) \to \eta_c(1S) + \gamma$. (h) $\eta_c(2S) \to h_c(1P) + \gamma$.

where $Q^2 = -q^2 = q_\perp^2$, and we have adopted $\arg \vec{q}_\perp = 0$ for simplicity. The coupling constant $E_1(0)$ is associated with dipole transition between the transversely polarized vector meson and the scalar meson:

$$E_1(0) = \frac{M_S^2 - M_V^2}{i\sqrt{2}} \sum_{s,\bar{s}} \int_0^1 \frac{\mathrm{d}x}{4\pi} \int \mathrm{d}^2 r_\perp (r_x + i r_y) \times \tilde{\psi}^{(\lambda=+1)*}_{s\bar{s}/V}(x, \vec{r}_\perp) \tilde{\psi}_{s\bar{s}/S}(x, \vec{r}_\perp), \tag{7}$$

in which $\tilde{\psi}(x, \vec{r}_\perp)$ is the transverse-coordinate-space LFWF. This expression resembles the nonrelativistic expression of the E1 transition. The TFF can also be extracted from the spatial current $\vec{J}_\perp$ [38,39]. Since the E1 transition is induced by the electric dipole, we adopt the charge density operator J^+, which has a smooth nonrelativistic limit as shown by Eq. (7).

Numerical results. The E1 widths associated with the ground-state scalar χ_{c0}, i.e., $\Gamma_{\chi_{c0} \to J/\psi\gamma}$, $\Gamma_{\psi(2S) \to \chi_{c0}\gamma}$, and $\Gamma_{\psi(3770) \to \chi_{c0}\gamma}$, and with the C-odd axial vector h_c, i.e., $\Gamma_{h_c \to \eta_c(1S)\gamma}$, $\Gamma_{\eta_c(2S) \to h_c\gamma}$, have been measured by several experiments [60–72] and compiled by PDG [51]. Some of the most recent measurements come from the CLEO and BES III collaborations. We compare our results[1] with the experimental data as well as the PDG values in Figs. 4(a)–4(d). Lattice QCD results [53,74–78] are also

[1]The values of the decay widths are provided in the Supplemental Material [73] of this paper.

compared in the same plots. Overall, our parameter-free results are in excellent agreement with the experimental data. Following our previous analyses for dilepton and diphoton and radiative transitions [38,39,43], we use the $N_{\max} = 8$ BLFQ LFWFs, whose UV scale $\Lambda_{\rm UV} = \kappa\sqrt{N_{\max}} = 2.8$ GeV matches the charmonium scale. We estimate the basis sensitivity as the difference between the $N_{\max} = 8$ and $N_{\max} = 16$ results.

The TFF $E_1(Q^2)$ provides further resolution of the system. Alas, the TFFs of these processes are not currently available from the experiments. We thus compare our BLFQ results with recent lattice simulations [53,74,75,78]. Figure 5(a) compares the TFFs of the transition between χ_{c0} and J/ψ as predicted by BLFQ and several lattice calculations [74,75,78]. Given the scattering of the lattice data from different groups, our BLFQ prediction is in reasonable agreement with these results, in particular at low Q^2. Our approach also provides access to moderately high Q^2, where the lattice simulations suffer from low statistics.

Similarly, Figs. 5(b) and 5(c) show the E1 TFFs of the processes $\psi(2S) \to \chi_{c0} + \gamma$ and $\psi(3770) \to \chi_{c0} + \gamma$, respectively. In nonrelativistic pictures, radiative transitions involving radially or angularly excited states, e.g., $\psi(2S)$ and $\psi(1D)$, are sensitive to the shape of the mesons wave function, e.g., the locations of the nodes. Our BLFQ predictions are again in good agreement with the lattice results [74], albeit the statistics of latter is limited at Q above 1 GeV. Figures 5(d)–5(f) show the E1 TFFs of $\chi_{c0}(3915)$ to the low-lying vector mesons, assuming that $\chi_{c0}(3915)$ is the $2P$ $c\bar{c}$ state. These predictions may serve as a benchmark for future investigation of $\chi_{c0}(3915)$.

The transitions involving the C-odd axial vector h_c are shown in Figs. 5(g) and 5(h). The TFF of the process $h_c \to \eta_c(1S) + \gamma$ is computed by Refs. [53,75] in lattice. Our results are in good agreement with Ref. [53] while deviating from [75]. Note that our E1 width of this process is in better agreement with the experimental data [68–72].

Summary and outlook. In this work, we investigate the E1 radiative transitions within the charmonium system using the basis light-front quantization approach. We derived the light-front wave function representation of the decay width as well as the transition form factors in the $|q\bar{q}\rangle$ Fock space. The wave functions adopted in this work come from fitting to the charmonium spectrum. Therefore, we are able to make parameter-free predictions for the E1 transitions. The results, including the widths and the form factors, are in excellent agreement with the experimental measurements as well as lattice simulations whenever available.

We also compute the E1 widths and the corresponding transition form factors of $\chi_{c0}(3915)$ by treating it as the $2P$ $c\bar{c}$ state. The obtained results are consistent with the recent measurement from Belle [52]. Further experimental measurements are required to discern the nature of this particle.

We note similar successes in describing the charmonium structures, viz., M1 transitions [39], two-photon transitions [38] as well as the decay constants [43] using the same set of light front wave functions. These applications provide confidence that the intrinsic structure of charmonium is accurately described by these BLFQ wave functions and lend support to the adopted phenomenological form of confinement [79]. We envision that further applications of the charmonium LFWFs will help to resolve the nonperturbative dynamics of the strong interaction in high-energy processes, such as the gluon distributions, generalized parton distributions, hadronic anomalous energy, etc., which are among the central goals of the forthcoming electron-ion colliders [80–90].

We also note the limitations of the model. We assume all charmonia are $c\bar{c}$ states, which is helpful to discern mesons' $c\bar{c}$ nature. However, higher Fock sector contributions must be incorporated to get a complete description of states, especially those above the open-charm threshold [57–59]. Another important issue is the choice of the current components beyond the traditional "good" current J^+, e.g., the transverse current [39]. The difference in quantities caused by different currents can be used to gauge the rotational symmetry violation, contributing to the overall model uncertainty. We will carry out those investigations in future works.

Acknowledgments. The authors acknowledge valuable discussions with P. Maris and X. Zhao. Y. L. is supported by the New faculty start-up fund of the University of Science and Technology of China. M. L. is supported by Xunta de Galicia (CIGUS accreditation), European Union ERDF, the Spanish Research State Agency under Project No. PID2020–119632 GB-I00, and European Research Council under Project No. ERC-2018-ADG-835105 YoctoLHC. This work was supported in part by the Chinese Academy of Sciences under Grant No. YSBR-101, and in part by the US Department of Energy (DOE) under Grant No. DE-SC0023692.

[1] N. Brambilla, S. Eidelman, B. K. Heltsley, R. Vogt, G. T. Bodwin, E. Eichten, A. D. Frawley, A. B. Meyer, R. E. Mitchell, V. Papadimitriou *et al.*, Eur. Phys. J. C **71**, 1534 (2011).

[2] N. Brambilla, S. Eidelman, C. Hanhart, A. Nefediev, C. P. Shen, C. E. Thomas, A. Vairo, and C. Z. Yuan, Phys. Rep. **873**, 1 (2020).

[3] H. X. Chen, W. Chen, X. Liu, Y. R. Liu, and S. L. Zhu, Rep. Prog. Phys. **86**, 026201 (2023).

[4] F. K. Guo, C. Hanhart, U. G. Meißner, Q. Wang, Q. Zhao, and B. S. Zou, Rev. Mod. Phys. **90**, 015004 (2018); **94**, 029901(E) (2022).

[5] S. Godfrey and N. Isgur, Phys. Rev. D **32**, 189 (1985).

[6] T. Barnes and S. Godfrey, Phys. Rev. D **69**, 054008 (2004).

[7] T. Barnes, S. Godfrey, and E. S. Swanson, Phys. Rev. D **72**, 054026 (2005).

[8] E. S. Swanson, Phys. Rep. **429**, 243 (2006).

[9] T. Barnes and E. S. Swanson, Phys. Rev. C **77**, 055206 (2008).

[10] M. R. Pennington and D. J. Wilson, Phys. Rev. D **76**, 077502 (2007).

[11] S. Godfrey and S. L. Olsen, Annu. Rev. Nucl. Part. Sci. **58**, 51 (2008).

[12] I. V. Danilkin and Y. A. Simonov, Phys. Rev. Lett. **105**, 102002 (2010).

[13] J. Ferretti, G. Galatà, and E. Santopinto, Phys. Rev. C **88**, 015207 (2013).

[14] P. G. Ortega, J. Segovia, D. R. Entem, and F. Fernández, Phys. Lett. B **778**, 1 (2018).

[15] R. Bruschini and P. González, J. High Energy Phys. 02 (2023) 216.

[16] F. K. Guo and U. G. Meissner, Phys. Rev. D **86**, 091501 (2012).

[17] S. L. Olsen, Phys. Rev. D **91**, 057501 (2015).

[18] Z. Y. Zhou, Z. Xiao, and H. Q. Zhou, Phys. Rev. Lett. **115**, 022001 (2015).

[19] G. L. Yu, Z. G. Wang, and Z. Y. Li, Chin. Phys. C **42**, 4 (2018).

[20] F. Gross, E. Klempt, S. J. Brodsky, A. J. Buras, V. D. Burkert, G. Heinrich, K. Jakobs, C. A. Meyer, K. Orginos, M. Strickland *et al.*, Eur. Phys. J. C **83**, 1125 (2023).

[21] A. B. Henriques, B. H. Kellett, and R. G. Moorhouse, Phys. Lett. **64B**, 85 (1976).

[22] K. Konigsmann, Phys. Rep. **139**, 243 (1986).

[23] O. Lakhina and E. S. Swanson, Phys. Rev. D **74**, 014012 (2006).

[24] E. Eichten, S. Godfrey, H. Mahlke, and J. L. Rosner, Rev. Mod. Phys. **80**, 1161 (2008).

[25] C. W. Zhao, G. Li, X. H. Liu, and F. L. Shao, Eur. Phys. J. C **73**, 2482 (2013).

[26] P. Guo, T. Yépez-Martínez, and A. P. Szczepaniak, Phys. Rev. D **89**, 116005 (2014).

[27] W. J. Deng, H. Liu, L. C. Gui, and X. H. Zhong, Phys. Rev. D **95**, 034026 (2017).

[28] E. Kou *et al.* (Belle-II Collaboration), Prog. Theor. Exp. Phys. **2019**, 123C01 (2019); **2020**, 029201(E) (2020).

[29] M. Hoferichter and P. Stoffer, J. High Energy Phys. 05 (2020) 159.

[30] X. Yao, Int. J. Mod. Phys. A **36**, 2130010 (2021).

[31] G. Ganbold, T. Gutsche, M. A. Ivanov, and V. E. Lyubovitskij, Phys. Rev. D **104**, 094048 (2021).

[32] K. H. Hong, H. C. Kim, and U. Yakhshiev, Prog. Theor. Exp. Phys. **2022**, 103D02 (2022).

[33] I. Babiarz, V. P. Goncalves, R. Pasechnik, W. Schäfer, and A. Szczurek, Phys. Rev. D **100**, 054018 (2019).

[34] F. Feng, Y. Jia, and W. L. Sang, Phys. Rev. Lett. **115**, 222001 (2015).

[35] F. Feng, Y. Jia, and W. L. Sang, Phys. Rev. Lett. **119**, 252001 (2017).

[36] S. Abreu, M. Becchetti, C. Duhr, and M. A. Ozcelik, J. High Energy Phys. 02 (2023) 250.

[37] J. Chen, M. Ding, L. Chang, and Y. x. Liu, Phys. Rev. D **95**, 016010 (2017).

[38] Y. Li, M. Li, and J. P. Vary, Phys. Rev. D **105**, L071901 (2022).

[39] M. Li, Y. Li, P. Maris, and J. P. Vary, Phys. Rev. D **98**, 034024 (2018).

[40] Yang Li, Heavy quarkonium light front wave functions from basis light-front quantization with a running coupling, Mendeley data, V2, 10.17632/cjs4ykv8cv.2 (2019).

[41] P. Maris, S. Jia, M. Li, Y. Li, S. Tang, and J. P. Vary, Proc. Sci. LC2019 (**2020**) 007 [arXiv:2002.06489].

[42] J. P. Vary, H. Honkanen, J. Li, P. Maris, S. J. Brodsky, A. Harindranath, G. F. de Teramond, P. Sternberg, E. G. Ng, and C. Yang, Phys. Rev. C **81**, 035205 (2010).

[43] Y. Li, P. Maris, and J. P. Vary, Phys. Rev. D **96**, 016022 (2017).

[44] L. Adhikari, Y. Li, M. Li, and J. P. Vary, Phys. Rev. C **99**, 035208 (2019).

[45] G. Chen, Y. Li, K. Tuchin, and J. P. Vary, Phys. Rev. C **100**, 025208 (2019).

[46] J. Lan, C. Mondal, M. Li, Y. Li, S. Tang, X. Zhao, and J. P. Vary, Phys. Rev. D **102**, 014020 (2020).

[47] T. Lappi, H. Mäntysaari, and J. Penttala, Phys. Rev. D **102**, 054020 (2020).

[48] I. Babiarz, R. Pasechnik, W. Schäfer, and A. Szczurek, Phys. Rev. D **107**, L071503 (2023).

[49] S. Leitão, A. Stadler, M. T. Peña, and E. P. Biernat, Phys. Rev. D **96**, 074007 (2017).

[50] C. S. Fischer, S. Kubrak, and R. Williams, Eur. Phys. J. A **51**, 10 (2015).

[51] R. L. Workman *et al.* (Particle Data Group), Prog. Theor. Exp. Phys. **2022**, 083C01 (2022).

[52] X. L. Wang *et al.* (Belle Collaboration), Phys. Rev. D **105**, 112011 (2022).

[53] J. J. Dudek, R. G. Edwards, and D. G. Richards, Phys. Rev. D **73**, 074507 (2006).

[54] S. D. Drell and T. M. Yan, Phys. Rev. Lett. **24**, 181 (1970).

[55] S. J. Brodsky, H. C. Pauli, and S. S. Pinsky, Phys. Rep. **301**, 299 (1998).

[56] J. Carbonell, B. Desplanques, V. A. Karmanov, and J. F. Mathiot, Phys. Rep. **300**, 215 (1998).

[57] J. Lan, K. Fu, C. Mondal, X. Zhao, and J. P. Vary (BLFQ Collaboration), Phys. Lett. B **825**, 136890 (2022).

[58] S. Xu, C. Mondal, X. Zhao, Y. Li, and J. P. Vary, arXiv:2209.08584.

[59] B. Pasquini, S. Rodini, and S. Venturini (MAP (Multi-dimensional Analyses of Partonic distributions) Collaboration), Phys. Rev. D **107**, 114023 (2023).

[60] N. E. Adam *et al.* (CLEO Collaboration), Phys. Rev. Lett. **94**, 232002 (2005).
[61] M. Ablikim *et al.* (BESIII Collaboration), Phys. Rev. D **96**, 032001 (2017).
[62] J. S. Whitaker, W. M. Tanenbaum, G. S. Abrams, M. S. Alam, A. Boyarski, M. Breidenbach, W. Chinowsky, R. DeVoe, G. J. Feldman, C. E. Friedberg *et al.*, Phys. Rev. Lett. **37**, 1596 (1976).
[63] C. J. Biddick, T. H. Burnett, G. E. Masek, E. S. Miller, J. G. Smith, J. P. Stronski, M. K. Sullivan, W. Vernon, D. H. Badtke, B. A. Barnett *et al.*, Phys. Rev. Lett. **38**, 1324 (1977).
[64] J. Gaiser, E. D. Bloom, F. Bulos, G. Godfrey, C. M. Kiesling, W. S. Lockman, M. Oreglia, D. L. Scharre, C. Edwards, R. Partridge *et al.*, Phys. Rev. D **34**, 711 (1986).
[65] S. B. Athar *et al.* (CLEO Collaboration), Phys. Rev. D **70**, 112002 (2004).
[66] R. A. Briere *et al.* (CLEO Collaboration), Phys. Rev. D **74**, 031106 (2006).
[67] M. Ablikim *et al.* (BESIII Collaboration), Phys. Lett. B **753**, 103 (2016).
[68] M. Ablikim *et al.* (BESIII Collaboration), Phys. Rev. D **86**, 092009 (2012).
[69] M. Ablikim *et al.* (BESIII Collaboration), Phys. Rev. D **106**, 072007 (2022).
[70] S. Dobbs *et al.* (CLEO Collaboration), Phys. Rev. Lett. **101**, 182003 (2008).
[71] M. Ablikim *et al.* (BESIII Collaboration), Phys. Rev. Lett. **104**, 132002 (2010).
[72] J. L. Rosner *et al.* (CLEO Collaboration), Phys. Rev. Lett. **95**, 102003 (2005).
[73] See the Supplemental Material at http://link.aps.org/supplemental/10.1103/PhysRevD.109.L031902 for the values of the decay widths.
[74] J. J. Dudek, R. Edwards, and C. E. Thomas, Phys. Rev. D **79**, 094504 (2009).
[75] Y. Chen, D. C. Du, B. Z. Guo, N. Li, C. Liu, H. Liu, Y. B. Liu, J. P. Ma, X. F. Meng, Z. Y. Niu *et al.*, Phys. Rev. D **84**, 034503 (2011).
[76] D. Becirevic and F. Sanfilippo, J. High Energy Phys. 01 (2013) 028.
[77] N. Li, C. C. Liu, and Y. J. Wu, Europhys. Lett. **133**, 11001 (2021).
[78] J. Delaney, C. E. Thomas, and S. M. Ryan, arXiv:2301.08213.
[79] S. J. Brodsky, G. F. de Teramond, H. G. Dosch, and J. Erlich, Phys. Rep. **584**, 1 (2015).
[80] A. Cisek, W. Schäfer, and A. Szczurek, J. High Energy Phys. 04 (2015) 159.
[81] G. Chen, Y. Li, P. Maris, K. Tuchin, and J. P. Vary, Phys. Lett. B **769**, 477 (2017).
[82] V. P. Gonçalves, M. V. T. Machado, B. D. Moreira, F. S. Navarra, and G. S. dos Santos, Phys. Rev. D **96**, 094027 (2017).
[83] E. C. Aschenauer, S. Fazio, J. H. Lee, H. Mantysaari, B. S. Page, B. Schenke, T. Ullrich, R. Venugopalan, and P. Zurita, Rep. Prog. Phys. **82**, 024301 (2019).
[84] V. P. Goncalves, D. E. Martins, and C. R. Sena, Nucl. Phys. **A1004**, 122055 (2020).
[85] D. P. Anderle, V. Bertone, X. Cao, L. Chang, N. Chang, G. Chen, X. Chen, Z. Chen, Z. Cui, L. Dai *et al.*, Front. Phys. (Beijing) **16**, 64701 (2021).
[86] R. Abdul Khalek, A. Accardi, J. Adam, D. Adamiak, W. Akers, M. Albaladejo, A. Al-bataineh, M. G. Alexeev, F. Ameli, P. Antonioli *et al.*, Nucl. Phys. **A1026**, 122447 (2022).
[87] H. Mäntysaari and J. Penttala, J. High Energy Phys. 08 (2022) 247.
[88] R. Abir, I. Akushevich, T. Altinoluk, D. P. Anderle, F. P. Aslan, A. Bacchetta, B. Balantekin, J. Barata, M. Battaglieri, C. A. Bertulani *et al.*, arXiv:2305.14572.
[89] A. Accardi, P. Achenbach, D. Adhikari, A. Afanasev, C. S. Akondi, N. Akopov, M. Albaladejo, H. Albataineh, M. Albrecht, B. Almeida-Zamora *et al.*, arXiv:2306.09360.
[90] I. Babiarz, V. P. Goncalves, W. Schäfer, and A. Szczurek, Phys. Lett. B **843**, 138046 (2023).